Autoionization of N_2

Carolyn Duzy* and R. Stephen Berry

Department of Chemistry and The James Franck Institute, The University of Chicago, Chicago, Illinois 60637
(Received 16 September 1975)

Autoionization of N_2 has been investigated theoretically, for the energy region between the threshold for production of N_2^+ in its ground state, and the threshold for production of the first excited state of N_2^+. Both vibrationally induced and electronically induced autoionization were studied. Rates for the former process, originating with Rydberg states in the $np\sigma_u\,{}^1\Sigma_u^+(v'>0)$ and $np\pi_u\,{}^1\Pi_u\,(v'>0)$ series, are of order 10^{10} sec^{-1} or slower, and correspond to linewidths of 0.2 cm^{-1} or less. Electronically induced autoionization is faster, with typical rates 10^{11}–10^{12} sec^{-1}, corresponding to linewidths of 0.5–5 cm^{-1}, consistent with observations.

I. INTRODUCTION

In the preceding paper (henceforth referred to as Paper I), the process of direct photoionization of N_2 was discussed. For the energy region just above the first ionization threshold, however, direct photoionization is responsible for less than half of the total observed ionization. The remainder is due to the interaction of bound states with the continuum, a process known as autoionization. It is autoionization that is discussed in this paper.

Autoionization can be thought of as a two-step process. First, a molecule is raised into an excited, bound state, which exists for some finite time. This state then couples to the continuum and ionization occurs. The essence of autoionization is the existence of degrees of freedom among which energy may be temporarily distributed, and from which it eventually passes to a mode that leads to a continuum state and, hence, to an irreversible decay. The internal mode may be electronic excitation, vibration, rotation, or even spin angular momentum of electrons or nuclei. The *upper* limit for any autoionization rate is set by the characteristic frequency of the "storage" degree of freedom.

Two mechanisms for this coupling are considered in this paper. They are vibronic coupling in which molecular vibration is the storage mode, and configuration interaction corresponding to storage in electronic excitation. Vibronic coupling can be thought of as arising from the breakdown of the Born–Oppenheimer approximation. In terms of a computation, the effect of the nuclear kinetic energy operator on the electronic wavefunction, which is normally neglected in the calculation of the zero-order function, can no longer be ignored, and it is the inclusion of interaction that lets us represent the mixing of bound and continuum states. In vibronic coupling, a vibrationally and electronically excited bound state of a molecule interacts with the continuum of a free electron and an ion with less vibrational excitation. Configuration interaction occurs because the correlation effects between electrons, which are disregarded in the calculation of the zero-order "bound" state, actually have an appreciable effect on the system. In the type of configuration interaction of interest to us, a doubly electronically excited state of a molecule interacts with the continuum corresponding to a free electron leaving the ground state of the ion.

Specifically, we will consider the effect of these two kinds of autoionization on the portion of the photoelectron spectrum between the first ionization threshold of N_2^+ (15.58 eV.) and the threshold for the production of the first excited state of N_2^+ (16.69 eV.). The rates for these processes will be calculated and the results compared with the photoionization spectrum obtained by Dehmer and Chupka,[1] and absorption data reported to us by Carroll.[2]

A complete description of the electronic configuration and the symmetries of the various states of N_2 and N_2^+ is given in Paper I. For the processes considered here, only the outer two valence orbitals are of interest. They are of symmetries σ_g and π_u, the σ_g being the highest in energy. The ground state of N_2 is a ${}^1\Sigma_g^+$ state, so that of N_2^+ is a ${}^2\Sigma_g^+$ state. All processes considered here start in the former state and finish in the latter.

Selection rules for dipole radiation require that an electron in a σ_g orbital can be excited into a σ_u or π_u state and a π_u electron into a σ_g, π_g, or δ_g state. These excited states can, of course, be either bound or part of the continuum. Some of the bound states produced by these excitations may interact with a free electron and N_2^+ in the ${}^2\Sigma_g^+$ state causing autoionization. Table I contains a classification of the Rydberg states which can autoionize, the continuum states to which they couple and the autoionization mechanism responsible for

TABLE I. Autoionizing Rydberg states of N_2, leading to $N_2^+(X\,{}^2\Sigma_g^+) + e$.

Bound state	Bound orbital	Continuum wave	Mechanism
${}^{1,3}\Sigma_u^+$	$p\sigma_u$	$p\sigma_u$	Vibronic coupling
${}^{1,3}\Pi_u$	$p\pi_u$	$p\pi_u$	Vibronic coupling
${}^{1,3}\Sigma_u^+$	$p\sigma_u$	$s\sigma_g$, $d\sigma_g$	Rotational–electronic coupling
${}^{1,3}\Pi_u$	$p\pi_u$	$d\pi_g$	Rotational–electronic coupling
${}^{1,3}\Pi_u$	$s\sigma_g$	$p\pi_u$	Configuration interaction
${}^{1,3}\Pi_u$	$d\sigma_g$	$p\pi_u$	Configuration interaction
${}^{1,3}\Sigma_u$	$d\pi_g$	$p\sigma_u$	Configuration interaction
${}^{1,3}\Delta_u$	$d\pi_g$	$p\sigma_u$	Configuration interaction
${}^{1,3}\Pi_u$	$d\delta_g$	$p\pi_u$	Configuration interaction
${}^{1,3}\Phi_u$	$d\delta_g$	$p\pi_u$	Configuration interaction

the interaction. In the present treatment, we neglect rotation–electronic coupling because there is no apparent need to invoke this mechanism for autoionization of N_2. The appropriate procedure would follow the method of Fano and Dill.[3]

II. THEORY AND METHOD

A description of the autoionization matrix elements is now in order. For diatomic molecules, the nuclear kinetic energy operator, T_R, can be expressed as

$$T_R \cong -\frac{1}{2M}\frac{d^2}{dR^2}+\frac{G^2}{2MR^2}, \tag{1}$$

where M is the reduced mass of the nuclei and G is the angular momentum of the nuclei. The first term gives rise to electronic–vibrational coupling and the second to electronic–rotational coupling. Following the argument given by Berry,[4] when vibrationally induced autoionization may occur, it will generally be faster than rotationally induced autoionization, although exceptions may occur, especially if large Δv transitions compete with favorable ΔJ transitions. Judging from the data,[1,2] for the purposes of this paper, processes involving the second term of T_R can be neglected. It should be noted, however, that in some cases, for example in H_2 just above the ionization threshold,[5] the second term does make a significant contribution to autoionization.

The interaction matrices of the first term of Eq. (1) are of the following form:

$$\langle\Psi_f|T_R|\Psi_i\rangle = -\frac{1}{2M}\left[2\left\langle\chi_f\left(\Psi_f\left|\frac{d\Psi_i}{dR}\right.\right)\frac{d\chi_i}{dR}C\right\rangle + \left\langle\chi_f\left(\Psi_f\left|\frac{d^2\Psi_i}{dR^2}\right.\right)\chi_i C\right\rangle\right]. \tag{2}$$

$\langle\,\rangle$ indicates integration over internuclear distance and $(\,)$ over the coordinates of the electron involved in the transition; Ψ_i is the initial orbital of the active electron, Ψ_f is the final, continuum state of the outgoing electron, χ_i is the initial vibrational wave function of the N_2 molecule, χ_f is the final vibrational wavefunction of the N_2^+ ion, and C is the overlap integral of the remaining occupied orbitals.

We assume that, in the second term in brackets on the right hand side of Eq. (2), the electronic factor in the integral varies slowly with internuclear distance, and that the vibrational wavefunctions are nearly orthogonal; these assumptions justify the supposition that this term is much smaller than the first term and can be neglected. This assumption has been made for autoionization in H_2[6] and appears to be valid for that molecule, except when configuration mixing among bound orbitals varies rapidly with internuclear distance (as with $s\sigma$ and $d\sigma$ orbitals).

One identity is useful in evaluating the vibronic coupling matrix elements. From the commutator of $\mathcal{H}_0$, the unperturbed (Born–Oppenheimer) Hamiltonian, and d/dR, where R is the internuclear distance, the following relationship can be derived, when Ψ_i and Ψ_f are eigenstates of $\mathcal{H}$:

$$\left(\Psi_f\left|\frac{\partial\Psi_i}{\partial R}\right.\right) = \frac{1}{\epsilon_i-\epsilon_f}\left(\Psi_f\left|\frac{dV}{dR}\right|\Psi_i\right), \tag{3}$$

where $\mathcal{H} = -1/2\mu\nabla_r^2 + V(r,R)$ and the ϵ_j's are the electronic energies of the states. The major advantages of this expression are that the matrix elements dV/dR approach zero at considerably smaller values of r, the radial coordinate of the active electron, than do the corresponding matrix elements involving $d\Psi_i/dR$ and that only one differentiation, dV/dR, is needed to evaluate matrix elements for all possible initial states of the system.

The operator responsible for configuration interaction is $\sum_j e^2/r_{1j}$, where $r_{1j} = |r_1 - r_j|$, the distance between electron 1, the active electron, and the other electrons in the molecule. In order to calculate matrix elements involving this operator $1/r_{1j}$ is expanded in terms of spherical harmonics.

It can be seen that there are two matrix elements involving the $1/r_{12}$ operator for every transition studied. They are the Coulomb integral

$$\left[\Psi_{a'}(1)\Psi_{b'}(2)\left|\frac{1}{r_{12}}\right|\Psi_a(1)\Psi_b(2)\right], \tag{4}$$

and the exchange integral

$$\left[\Psi_{a'}(2)\Psi_{b'}(1)\left|\frac{1}{r_{12}}\right|\Psi_a(1)\Psi_b(2)\right], \tag{5}$$

where integration is over the coordinates of electrons 1 and 2. Both integrals make a significant contribution to the transition rates for configuration interaction, so both are evaluated in this paper.

Once the matrix elements have been evaluated for either coupling operator O, the rates for autoionization can be calculated using the Wentzel Golden Rule expression

$$\text{rate} = \frac{2\pi}{\hbar}|\langle\Psi_f|O|\Psi_i\rangle|^2\rho, \tag{6}$$

where ρ is the density of final continuum states.

The method used to calculate the electronic and vibrational wavefunctions which appear in the autoionization matrix elements is described in detail in Sec. II of Paper I. A brief summary description of the calculation of the electronic wavefunctions of the active electron is in order at this time. The charge density due to the nuclei and the thirteen "inactive" electrons of the molecule was found and expanded in spherical harmonics. The first terms of the expansion consist of a spherically symmetric (monopole) Coulombic contribution and a monopole contribution from a local approximation to the exchange potential. These are denoted as V_{OC} and V_{OE}, respectively. Because N_2 is homonuclear, the next term in the expansion is the electrostatic quadrupole term, denoted by V_{2C}. The continuum wavefunctions were calculated numerically using $V_{OC} + V_{OE}$ as the potential in the Schrödinger equation. The Rydberg wavefunctions were calculated to zero order using $V_{OC} + V_{OE}$ as the potential. V_{2C} was then used as a perturbation to calculate the first-order Rydberg

wavefunctions and it is these wavefunctions which are used in all calculations in this paper. Hence we include $(\ell_0\ell')$ coupling to the lowest order of terms in V_{2C} for the bound states but we omit terms in V_{2E} and higher tensorial components of the potential, and neglect partial-wave coupling in the continuum. Paper I also contains a discussion of the first stage of the autoionization process, namely, excitation of molecular N_2 from its ground state to a Rydberg state. Table IV of that paper lists the oscillator strengths for excitation to the autoionizing states.

Before the results for the autoionization rates are given, some mention should be made of possible competing mechanisms. These are fluorescence, predissociation, and interaction with other Rydberg states of nearly degenerate energy. None of these are likely to interfere greatly with autoionization in the energy range of interest in this paper.

Fluorescence rates to the ground state of N_2 were calculated for some of the autoionizing Rydberg states. In all cases they were five or six orders of magnitude slower than the corresponding rates for autoionization. It therefore seems unlikely that even the total fluorescence rate to all possible lower states would seriously compete with autoionization as a decay mode. No appreciable predissociation has been experimentally observed in this energy range, so it seems reasonable to disregard this decay mechanism. Berry and Nielsen,[6] in their work on H_2, found that relatively little Rydberg–Rydberg mixing occurred; occasional instances of Rydberg → Rydberg′ → continuum coupling do occur for H_2, and play an important role for states that would autoionize only very slowly by "direct" transition. In N_2 direct autoionization turns out to be fairly rapid, so we have neglected configuration interaction coupling among bound Rydberg states, as a contributor to the overall autoionization rates.

III. RESULTS

Rates of autoionization by vibronic coupling are listed in Table II. Transitions from Rydberg states with vibrational quantum number of 1–4 to continuum states with vibrational quantum numbers 0, 1, and 2 are considered. The potential used in calculating these rates is $V_{OC} + V_{OE} + V_{2C}$. We found that the V_{2C} term changed the rates by a factor of 1.1 to 3, with the amount of change following no discernible pattern.

It should be noted that for $\Delta v \leq -3$, the rates for vibronic coupling first decrease and then increase with increasing principle quantum number. This is caused, as in the case of the photoabsorption oscillator strengths discussed in Paper I, by destructive interference among the partial waves which contribute to the Rydberg wavefunctions. This effect is not as marked as in the oscillator strengths, since it is offset by a decrease, with increasing energy, in the amplitude of the continuum wavefunctions contained in the matrix elements.

Autoionization rates for vibronic coupling are plotted in Fig. 1, to show the dependence of these rates on energy, principle quantum number of the initial Rydberg state, and the change in the vibrational quantum number of the core.

The rates for autoionization by configuration interaction are given in Table III, and shown in Fig. 2. Because calculations of this sort require considerable computer time, only rates involving transitions between the ground vibrational states of the molecule and ion were calculated. A rough estimate of the rates for transitions with $\Delta v \neq 0$ can be obtained by assuming that the electronic contributions can be factored out, so that the rates would be proportional to the Franck–Con-

TABLE II. Autoionization rates for vibronic coupling.

A. $np\sigma$										
v	Δv	$n=4$	5	6	7	8	9	10	10	12[a]
0	−1	···	···	···	···	0.418(11)	0.624(10)	0.411(10)	0.130(10)	0.385(9)
0	−2	···	···	0.227(10)	0.141(10)	0.781(9)	0.274(9)	0.897(8)	0.113(8)	0.332(8)
0	−3	···	0.875(9)	0.180(9)	0.557(8)	0.159(8)	0.291(7)	0.882(5)	0.958(6)	0.388(8)
0	−4	···	0.587(8)	0.349(7)	0.324(7)	0.343(6)	0.207(5)	0.151(7)	0.381(8)	0.107(9)
1	−1	···	···	···	···	···	0.141(11)	0.137(11)	0.288(10)	0.591(9)
1	−2	···	···	0.605(10)	0.257(10)	0.710(9)	0.328(9)	0.142(9)	0.100(9)	0.103(9)
1	−3	···	0.333(10)	0.686(9)	0.219(9)	0.628(8)	0.684(7)	0.147(7)	0.430(7)	0.328(9)
2	−1	···	···	···	···	···	0.236(11)	0.173(11)	0.468(10)	0.173(10)
2	−2	···	···	0.105(11)	0.416(10)	0.155(10)	0.712(9)	0.815(8)	0.238(9)	0.199(10)
B. $np\pi$										
0	−1	···	···	···	···	0.892(11)	0.723(11)	0.517(11)	0.259(11)	0.598(10)
0	−2	···	···	0.713(10)	0.485(10)	0.323(10)	0.237(10)	0.682(9)	0.285(9)	0.255(9)
0	−3	···	0.582(9)	0.420(9)	0.360(9)	0.270(9)	0.212(9)	0.171(9)	0.656(8)	0.485(8)
0	−4	0.794(5)	0.271(8)	0.214(8)	0.153(8)	0.143(8)	0.111(8)	0.703(7)	0.362(7)	0.113(7)
1	−1	···	···	···	···	0.197(12)	0.159(12)	0.116(12)	0.563(11)	0.170(11)
1	−2	···	···	0.195(11)	0.131(11)	0.103(11)	0.962(10)	0.828(10)	0.661(10)	0.231(10)
1	−3	···	0.224(10)	0.68(10)	0.131(10)	0.105(10)	0.835(9)	0.660(9)	0.250(9)	0.193(9)
2	−1	···	···	···	···	0.332(12)	0.260(12)	0.194(12)	0.906(11)	0.342(11)
2	−2	···	···	0.355(11)	0.221(11)	0.195(11)	0.147(11)	0.123(11)	0.400(10)	0.127(10)

[a]Powers of 10 are in parentheses.

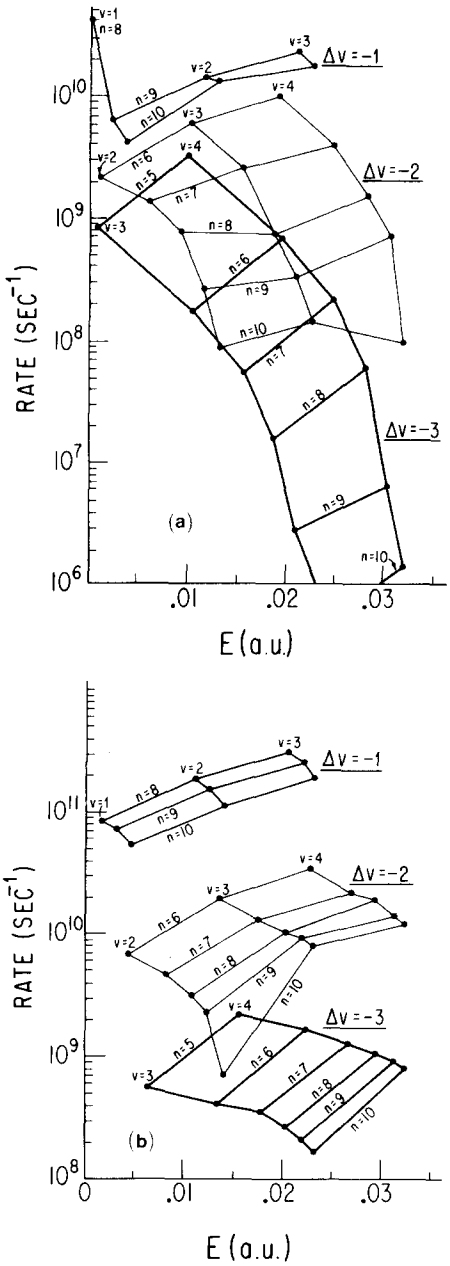

FIG. 1. Vibronic autoionization rates for N_2, leading to N_2^+ $(^2\Sigma_g^+)+e$; (a) $np\sigma$ Rydberg series; (b) $np\pi$ Rydberg series. Dots represent processes from particular initial Rydberg states; principal and vibrational quantum numbers n and v of those states are written in and the lines connect points associated with the same Δv. The energy on the abscissa is taken relative to the I. P.

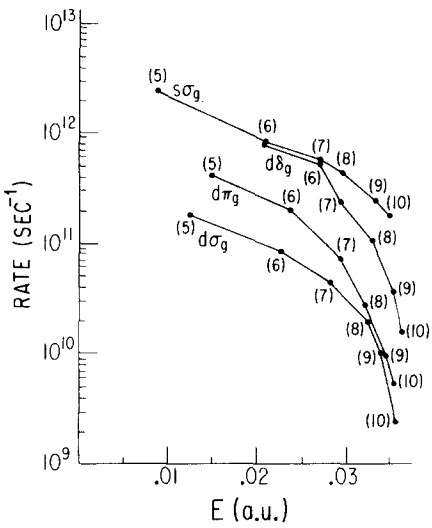

FIG. 2. Electron-correlation-induced autoionization rates for Rydberg states in the series converging to $N_2^+(A^2\,\Pi_u)+e$. Parenthesized numbers are the principal quantum numbers of the autoionizing states. The zero of energy is the I. P. of N_2.

don factors we have calculated from our vibrational wavefunctions. On the basis of the F–C factors, it would appear that the rates decrease approximately an order of magnitude for each increase in $|\Delta v|$.

One rather surprising conclusion can be drawn from the rates and oscillator strengths calculated in this paper and Paper I. It appears that states which couple to the continuum by vibronic coupling make very little contribution to the total ionization yield and that configuration interaction is by far more important in the energy region just above the first ionization threshold. This is primarily a consequence of the magnitudes of the oscillator strengths for excitation to the states involved in autoionization, (Table III of Paper I), rather than of the autoionization rates. For vibronic coupling, the states that make the greatest contribution to the photoionization spectrum are those with $v' = 1$ and $n \geq 8$; for configuration interaction the $ns\sigma_g$ state with $v' = 0$ and $n \geq 5$ are most important. The oscillator strengths for the $s\sigma_g$ states are roughly two orders of magnitude greater than those for the states involved in vibronic coupling. This suggest that very little evidence of vibronic coupling should be seen in the photoionization spectrum.

The experimental observations of the photoionization spectrum by Dehmer and Chupka[1] support this conclusion. The peaks for the $np\sigma_u$ and $np\pi_u$ states are just barely discernible, except for the $n = 9$ states, which are obscured by a large peak, and $n = 11$ states, which seem to be missing entirely. The peaks for the $ns\sigma_g$ states, on the other hand, are all present at exactly the predicted energies and they account for a major portion of the total cross section due to autoionization. Sections of this spectrum, with our calculated wavelengths, are shown in Fig. 3.

TABLE III. Autoionization rates for configuration interaction.

n	$ns\sigma$	$nd\sigma$	$nd\pi$	$nd\delta$[a]
5	0.247(13)	0.189(12)	0.420(12)	0.892(12)
6	0.821(12)	0.855(11)	0.223(12)	0.527(12)
7	0.592(12)	0.431(11)	0.712(11)	0.254(12)
8	0.447(12)	0.196(11)	0.286(11)	0.109(12)
9	0.251(12)	0.998(10)	0.945(10)	0.341(11)
10	0.180(12)	0.508(10)	0.256(10)	0.153(11)
11	0.134(12)	0.281(10)	0.551(9)	0.323(10)
12	0.933(11)	0.205(10)	0.529(10)	0.916(9)

[a]Powers of 10 are in parentheses.

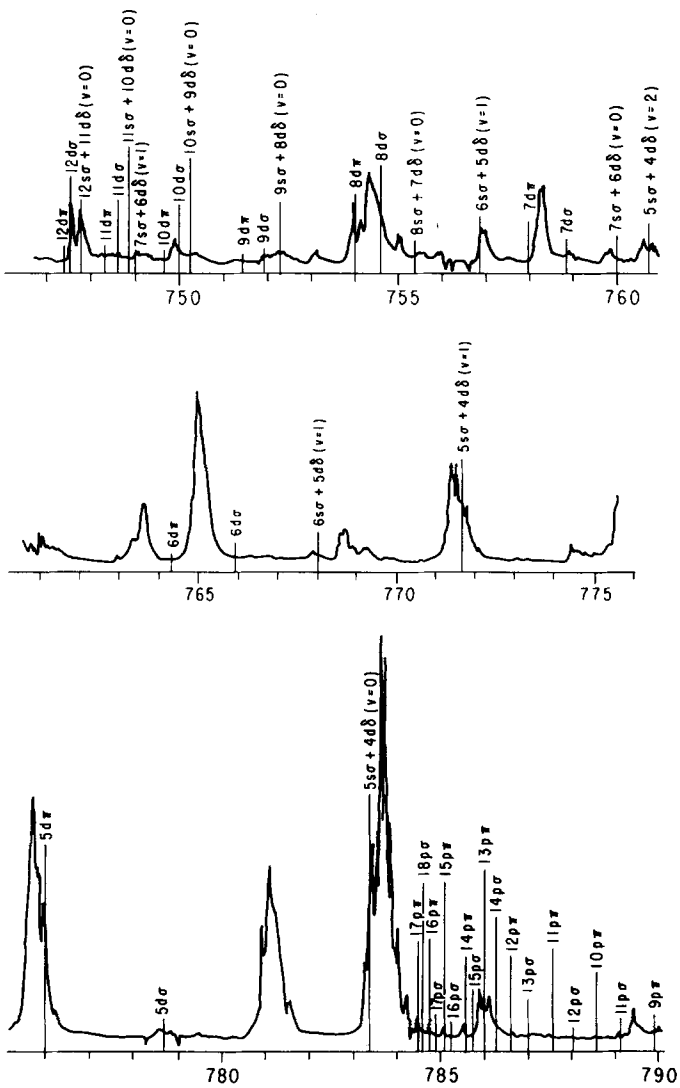

FIG. 3. Photoionization spectrum of N_2, with our computed transition energies indicated by vertical lines and labels. Values of the transition energies to $np\sigma$ and $np\pi$ states with $n > 12$ were obtained from extrapolations of our computed quantum defects. All computed $p\sigma$ and $p\pi$ levels shown here have $v' = 1$, and $d\sigma$ and $d\pi$ levels have $v = 0$. We are informed by an anonymous referee that the dips in the photoionization curve at 779 and 756.5 Å are "undoubtedly artifacts resulting from emission lines in the light source and should be removed."

The best comparison that can be made to date between experimental and theoretical lifetimes is based on the optical spectra obtained by Carroll (as reported to us).[2] Carroll finds that the series $[N_2^+ A\,^2\Pi_u] n\sigma_g$, $^1\Pi_u$, and the corresponding series of $^3\Pi_u$ states are strong and diffuse. These are the series called $o_n(v')$ and $O_n(v')$,[7-9] respectively, throughout earlier work on these series. (These series can decay by electronically induced autoionization). The "c series" of $[N_2^+ X^2\Sigma_g^+]\, np\pi_u$, $^1\Pi_u$ levels[10] appears much more weakly than the o series, and, where the bands are free of interference from the o series, display rotational structure. Carroll informs us, for example, that the c_{11} (1) band has broadening of less than about 1 cm^{-1}. We estimate an autoionization rate of about 2.6×10^{10} sec^{-1} for the $11\pi(v' = 1)\,^1\Pi_u$ Rydberg state, which corresponds to a linewidth of 0.18 cm^{-1}, according to the uncertainty relation, rate $= (\Delta t)^{-1} = 2\pi c\, \Delta v(cm^{-1})$. The implication of the calculations for the vibronically autoionized states is that the dominant mode of decay is indeed autoionization, rather than radiation, so long as $\Delta v \leq -2$ or -3. However, the linewidths, even for the Rydberg states that autoionize most rapidly by this mechanism, will be less than the spacing of rotational levels. Hence our calculated rates for the c series are entirely consistent with Carroll's observation of rotational structure in these bands. We do expect to see a few states, such as the $4p\pi_u(v' = 4)\,^1\Pi_u$, decay by radiation rather than autoionization because the electron loss process can only occur by the transfer of four vibrational quanta. There are few examples, if any, in which radiation and autoionization have comparable rates. As in H_2,[6] the calculations bear out the general vibrational propensity rule for the relationship between the heirarchy of rates and the number of vibrational quanta being transferred.

Returning to o series, we predict that the rates of decay of the $ns\sigma$ levels should be in the order of 10^{11}–10^{12} sec^{-1}, which appears to be consistent with the data of Carroll[2] and of Dehmer and Chupka,[1] at the qualitative level of analysis to which these studies have thus far been brought.

There are several strong unidentified lines in the spectrum of Fig. 3. These lines are presumably built on cores of the second and higher excited states of N_2^+ and, therefore, cannot be predicted from our calculations, which treat only the ground and first excited states of N_2^+.

At the outset of this work, we speculated that the Beutler–Fano line shape[11] might be used to distinguish among mechanisms of autoionization. This would be the case if, for example, electronically induced autoionization and vibronically induced autoionization led to line shapes characterized by different signs of the asymmetry parameter q.[12] We have evaluated lineshapes for both mechanisms; unfortunately for identification purposes, the q parameters are large and positive regardless of the mechanism of decay. Average computed values of q are as follows: for $p\sigma_u$ levels, 15.2; for $p\pi_u$, 20.9 (these two being the levels decaying by vibrationally induced autoionization); for $s\sigma_g$, 53.8; for $d\sigma_g$, 46.3; for $d\pi_g$, 3.24, and for $d\delta_g$, 41.8. Note that the interpretation of experimental line shapes ultimately rests on resolution of rotational levels; this has not been achieved for most spectral lines.

ACKNOWLEDGMENTS

We would like to express our thanks to Dr. P. K. Carroll, Dr. P. M. Dehmer, and Dr. W. A. Chupka, for sharing their results with us prior to publication, and to Dr. Dehmer and Dr. Chupka for allowing us to reproduce portions of their spectrograms. This work was supported under a grant from the National Science Foundation. Portions of the work were carried out at the Aspen Center for Physics, whose hospitality R. S. B. wishes to acknowledge.

*Present address: Department of Chemistry, University of Toronto, Toronto, Canada.

[1]P. M. Dehmer and W. A. Chupka (private communication, to be published).
[2]P. K. Carroll (private communication, to be published).
[3]U. Fano and D. Dill, Phys. Rev. A **6**, 185 (1972).
[4]R. S. Berry, J. Chem. Phys. **45**, 1228 (1966).
[5]G. Herzberg and Ch. Jungen, J. Mol. Spectrosc. **41**, 425 (1972).
[6]R. S. Berry and S. E. Nielsen, Phys. Rev. A **1**, 383 (1970).
[7]P. K. Carroll and K. Yoshino, J. Chem. Phys. **47**, 3073 (1967).
[8]P. K. Carroll and C. P. Collins, Can. J. Phys. **47**, 563 (1969).
[9]P. K. Carroll and K. Yoshino, J. Phys. B **5**, 1614 (1972).
[10]P. K. Carroll, J. Chem. Phys. **58**, 3597 (1973).
[11]U. Fano, Phys. Rev. **124**, 1866 (1961).
[12]The line shape has the form $(q+E)^2/(1+E^2)$ in the formulation of Fano; E is the energy away from the resonance energy, measured in units of the linewidth $\Gamma/2$.